Probing the curvature and dark energy

Yungui Gong
College of Electronic Engineering, Chongqing University of Posts and Telecommunications, Chongqing 400065, China

Yuan-Zhong Zhang
CCAST (World Laboratory), P.O. Box 8730, Beijing 100080, China
Institute of Theoretical Physics, Chinese Academy of Sciences, P.O. Box 2735, Beijing 100080, China
(Received 15 March 2005; published 22 August 2005)

Two new one-parameter tracking behavior dark energy representations $\omega = \omega_0/(1+z)$ and $\omega = \omega_0 e^{z/(1+z)}/(1+z)$ are used to probe the geometry of the Universe and the property of dark energy. The combined type Ia supernova, Sloan Digital Sky Survey, and Wilkinson Microwave Anisotropy Probe data indicate that the Universe is almost spatially flat and that dark energy contributes about 72% of the matter content of the present universe. The observational data also tell us that $\omega(0) \sim -1$. It is argued that the current observational data can hardly distinguish different dark energy models to the zeroth order. The transition redshift when the expansion of the Universe changed from deceleration phase to acceleration phase is around $z_T \sim 0.6$ by using our one-parameter dark energy models.

DOI: 10.1103/PhysRevD.72.043518 PACS numbers: 98.80.Es, 98.80.Cq

I. INTRODUCTION

The type Ia supernova (SN Ia) data suggest that the Universe is dominated by dark energy [1–3]. Since 1998, many dark energy models have been proposed in the literature. The simplest dark energy model is the cosmological constant model. However, the smallness of the value of the observed cosmological constant has puzzled theoretical physicists for a long time. For a review of dark energy models, see, for example, Refs. [4,5]. Although there exist a lot of dark energy models, we are still not able to decide which model gives us the right answer and find out the nature of dark energy. From a theoretical point of view, perhaps the lack of understanding of quantum gravity is the main reason. To advance our understanding of dark energy, we may use observational data to probe the nature of dark energy. It is not practical to test every single dark energy model by using the observational data. Therefore, a model independent probe of dark energy is one of the best choices to study the nature of dark energy.

The usual model independent method is through parametrizing dark energy or the equation of state parameter $\omega(z)$ of dark energy. The simplest method is parametrizing $\omega(z)$ as a constant. To model the dynamical evolution of dark energy, we can parametrize $\omega(z)$ as the power law expansion $\omega(z) = \sum_{i=0}^{N} \omega_i z^i$ [6–9]. Recently, a simple two-parameter model $\omega(z) = \omega_0 + \omega_a z/(1+z)$ was extensively discussed [10–13]. Jassal, Bagla, and Padmanabhan later modified this two-parameter model as $\omega(z) = \omega_0 + \omega_a z/(1+z)^2$ [14]. More complicated forms of $\omega(z)$ were also discussed in the literature [15–19]. Instead of parametrizing $\omega(z)$, we can also parametrize the dark energy density itself, like a simple power law expansion $\Omega(z) = \sum_{i=0}^{N} A_i z^i$ [20–25] and the piecewise constant parametrization [26–29]. In [15], Gong used the SN Ia data to discuss some two-parameter representations of dark energy in a spatially flat cosmology. It was found that the SN Ia data marginally favored a phantomlike dark energy model. It was also found that the transition redshift $z_T \sim 0.3$. In this paper, we propose two one-parameter dark energy models $\omega = \omega_0/(1+z)$ and $\omega = \omega_0 e^{z/(1+z)}/(1+z)$ and we use the SN Ia, the Sloan Digital Sky Survey (SDSS), and the Wilkinson Microwave Anisotropy Probe (WMAP) data to probe the geometry of the Universe. We also compare these two models with two two-parameter dark energy models.

This paper is organized as follows. In Sec. II, we first use the ΛCDM model as an example to show the method of fitting the whole 157 gold sample of SN Ia data compiled in [30], the parameter A measured from the SDSS data [31], and the shift parameter $\mathcal{R}$ measured from the WMAP data [26,27] to a dark energy model. The parameter A is a dark energy model independent parameter found by Eisenstein *et al.* in [31] when they analyzed the large scale correlation function of a large spectroscopic sample of luminous, red galaxies for SDSS. It is related to the path from $z = 0$ to $z = 0.35$. $\mathcal{R}$ is the shift of the positions of the acoustic peaks in the angular power spectrum due to the effect of changing the values of Ω_{m0} and Ω_{k0} on the cosmic microwave background anisotropy. In Sec. III, we propose two new tracking behavior one-parameter dark energy representations $\omega = \omega_0/(1+z)$ and $\omega = \omega_0 e^{z/(1+z)}/(1+z)$. In Sec. IV, we fit the models to the observational data. In Sec. V, we fit two two-parameter parametrizations $\omega = \omega_0 + \omega_a z/(1+z)$ and $\omega = \omega_0 + \omega_a z/(1+z)^2$ to the observational data. In Sec. VI, we conclude the paper with some discussion.

*Electronic address: gongyg@cqupt.edu.cn

 © 2005 The American Physical Society

II. ΛCDM MODEL WITH CURVATURE

For the simplest ΛCDM model where the dark energy is the cosmological constant, i.e., $\rho = -p = \Lambda$, we have

$$H^2 = H_0^2[\Omega_{m0}(1+z)^3 + \Omega_{r0}(1+z)^4 - \Omega_{k0}(1+z)^2 + 1 - \Omega_{m0} - \Omega_{r0}], \tag{1}$$

where $\Omega_m(\Omega_r) = 8\pi G\rho_m(\rho_r)/3H_0^2$, $\Omega_{r0} = 8.35 \times 10^{-5}$ [32], and $\Omega_k = k/a^2H_0^2$. The parameters Ω_{m0} and Ω_{k0} are determined by minimizing

$$\chi^2 = \sum_i \frac{[\mu_{\rm obs}(z_i) - \mu(z_i)]^2}{\sigma_i^2} + \frac{(A - 0.469)^2}{0.017^2} + \frac{(\mathcal{R} - 1.716)^2}{0.062^2}, \tag{2}$$

where the extinction-corrected distance modulus $\mu(z) = 5\log_{10}(d_{\rm L}(z)/{\rm Mpc}) + 25$, the luminosity distance is

$$d_{\rm L}(z) = a_0(1+z)r(z) = \frac{a_0(1+z)}{\sqrt{|k|}}\,{\rm sinn}\left[\frac{\sqrt{|k|}}{a_0H_0}\int_0^z \frac{dz'}{E(z')}\right] = \frac{1+z}{H_0\sqrt{|\Omega_{k0}|}}\,{\rm sinn}\left[\sqrt{|\Omega_{k0}|}\int_0^z \frac{dz'}{E(z')}\right], \tag{3}$$

${\rm sinn}(\sqrt{|k|}x)/\sqrt{|k|} = \sin(x)$, x, $\sinh(x)$ if $k = 1, 0, -1$, the dimensionless Hubble parameter $E(z) = H(z)/H_0$, the parameter A is defined as [31]

$$A = \frac{\sqrt{\Omega_{m0}}}{0.35}\left[\frac{0.35}{E(0.35)}\frac{1}{|\Omega_{k0}|}{\rm sinn}^2\left(\sqrt{|\Omega_{k0}|}\int_0^{0.35}\frac{dz}{E(z)}\right)\right]^{1/3} = 0.469 \pm 0.017, \tag{4}$$

the shift parameter [26,27]

$$\mathcal{R} = \frac{\sqrt{\Omega_{m0}}}{\sqrt{|\Omega_{k0}|}}\,{\rm sinn}\left(\sqrt{|\Omega_{k0}|}\int_0^{z_{ls}}\frac{dz}{E(z)}\right) = 1.716 \pm 0.062, \tag{5}$$

$z_{ls} = 1089 \pm 1$ [32], and σ_i is the total uncertainty in the SN Ia data. In other words, we use the 157 gold sample SN Ia data compiled in [30], the parameter A measured from the SDSS data [31], and the shift parameter $\mathcal{R}$ measured from the WMAP data [26,27] to find out the parameters Ω_{m0} and Ω_{k0}. The nuisance parameter H_0 which appeared in Eq. (3) is marginalized over with a flat prior assumption. Since H_0 appears linearly in the form of $5\log_{10}H_0$ in χ^2, so the marginalization by integrating $\mathcal{L} = \exp(-\chi^2/2)$ over all possible values of H_0 is equivalent to finding the value of H_0 which minimizes χ^2 if we also include the suitable integration constant and measure function.

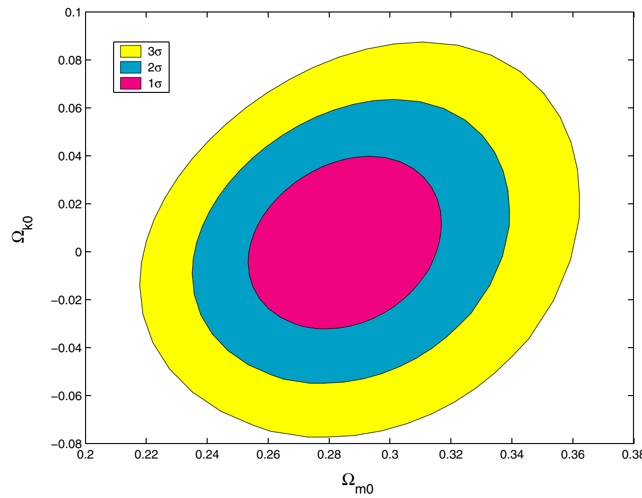

FIG. 1 (color online). The 1σ, 2σ, and 3σ contour plots of Ω_{m0} and Ω_{k0} for the model with the cosmological constant as dark energy.

The best fit parameters to the combined SN Ia, SDSS, and WMAP data are $\Omega_{m0} = 0.28 \pm 0.03$ and $\Omega_{k0} = 0.004 \pm 0.04$ with $\chi^2 = 177.14$. The contour plot of Ω_{m0} and Ω_{k0} is shown in Fig. 1.

III. ONE-PARAMETER PARAMETRIZATION

The main goal of this work is to study the geometry of the Universe and the property of dark energy by using observational data. In the introduction, we mentioned several different parametrizations. Those parametrizations have two or more parameters, so it is difficult to use those parametrizations to investigate the geometry of the Universe because we have to add two more cosmological parameters Ω_{m0} and Ω_{k0} to the model. Therefore, it is better that the parametrization has only one parameter so that the whole model has three cosmological parameters. Of course, this kind of parametrization assumed that the dark energy has evolution and it is not a cosmological constant.

Model 1: To make the parametrization physical, we look for tracking behavior representation, i.e., we require $\omega(z = \infty) = 0$. We first consider a simple one-parameter dark energy representation

$$\omega(z) = \frac{\omega_0}{1+z}. \tag{6}$$

At early times, $z \gg 1$, $\omega(z) \sim 0$. In the far future, $1 + z \to 0$ and $\omega(z) \to -\infty$. This simple parametrization has future singularity. The energy conservation equation of the dark energy can be written as

$$\frac{d\ln\rho}{dz} = \frac{3(1+\omega)}{1+z}. \tag{7}$$

The acceleration equation is

$$\frac{\ddot{a}}{a} = -\frac{4\pi G}{3}(\rho_m + 2\rho_r + \rho + 3p). \tag{8}$$

Combining Eqs. (6) and (7), we get

$$\rho = \rho_0(1+z)^3 \exp\left(\frac{3\omega_0 z}{1+z}\right). \tag{9}$$

It is obvious that $\rho \sim e^{3\omega_0}\rho_0(1+z)^3$ when $z \gg 1$ and $\rho \to \infty$ when $z \to -1$. At early times, the energy density looks like matter with effective $\Omega_{m0} = e^{3\omega_0}\Omega_0$. Here $\Omega = 8\pi G\rho/3H_0^2$ and $\Omega_0 = 1 + \Omega_{k0} - \Omega_{m0} - \Omega_{r0}$. This model may be thought of as a unified model of dark matter and dark energy. The sound speed of the model is

$$c_s^2 = \frac{\partial p}{\partial \rho} = \frac{2\omega_0(1+z) + 3\omega_0^2}{3(1+z)^2 + 3\omega_0(1+z)}. \tag{10}$$

So $c_{s0}^2 = (2\omega_0 + 3\omega_0^2)/(3 + 3\omega_0) \neq 0$. When $1 + z + \omega_0 > 0$ and $1 + z + 1.5\omega_0 < 0$, $c_{s0}^2 > 0$. For any unified theory of dark energy and dark matter, it was shown that the wave number k dependence of density perturbation growth due to the presence of a nonzero sound speed for a period of time produces unphysical oscillations or exponential blowup in the matter power spectrum [33–35]. Therefore this model as the unified model of dark matter and dark energy is not feasible. The model with interactions between dark energy and dark matter was discussed in [36].

Now we consider the model as a dark energy model. As we saw above, the dark energy behaves as ordinary matter at early times, we can interpret this as the tracking behavior, i.e., the dark energy tracked the matter at early times. The total effective matter density is $\Omega_{m0}^{\mathrm{eff}} = \Omega_{m0} + e^{3\omega_0}\Omega_0$, and we expect that $e^{3\omega_0}\Omega_0 \ll \Omega_{m0}$. Substitute Eqs. (6) and (9) into Eq. (8) and neglect the radiation contribution; we find that the transition redshift z_{T} satisfies the following equation:

$$(1+z)^3\left[\Omega_{m0} + \left(1 + \frac{3\omega_0}{1+z}\right)\Omega_0 \exp\left(\frac{3\omega_0 z}{1+z}\right)\right] = 0. \tag{11}$$

Model 2: Now we consider another one-parameter dark energy parametrization:

$$\omega(z) = \frac{\omega_0}{1+z} e^{z/(1+z)}. \tag{12}$$

For this model, $\omega(z) \sim 0$ when $z \gg 1$. The major difference between this model (12) and the model (6) is that $\omega(z) \to 0$ as $z \to -1$ for this model. These two models have almost the same behavior in the past and very different behavior in the future. Combining Eqs. (7) and (12), we get

$$\rho = \rho_0(1+z)^3 \exp(3\omega_0 e^{z/(1+z)} - 3\omega_0). \tag{13}$$

It is obvious that $\rho \sim e^{3\omega_0 e - 3\omega_0}\rho_0(1+z)^3$ when $z \gg 1$ and $\rho \sim e^{-3\omega_0}\rho_0(1+z)^3$ when $z \to -1$. At early times, the energy density looks like matter with effective $\Omega_{m0} = e^{3\omega_0 e - 3\omega_0}\Omega_0$, and it behaves like matter with effective $\Omega_{m0} = e^{-3\omega_0}\Omega_0$ in the far future, too. This model may also be thought as a unified model of dark matter and dark energy. The sound speed of the model is

$$c_s^2 = \frac{\partial p}{\partial \rho} = \frac{2\omega_0(1+z)e^{z/(1+z)} + \omega_0(1 + 3\omega_0 e^{z/(1+z)})e^{z/(1+z)}}{3(1+z)^2 + 3\omega_0 e^{z/(1+z)}}. \tag{14}$$

So $c_{s0}^2 = \omega_0 < 0$ and it also produces exponential blowup in the matter power spectrum. This model as the unified model of dark matter and dark energy is not feasible also. Again we consider this model as a dark energy model. One key feature of this model is that the model behaves like matter both in the past and the future. The Universe will expand with deceleration in the future. In the past, the dark energy tracked the matter. The total effective matter density is $\Omega_{m0}^{\mathrm{eff}} = \Omega_{m0} + e^{3\omega_0(e-1)}\Omega_0$, and we expect that $e^{3\omega_0(e-1)}\Omega_0 \ll \Omega_{m0}$. Substitute Eqs. (12) and (13) into Eq. (8) and neglect the radiation contribution; we find that the transition redshift z_{T} satisfies the following equation:

$$(1+z)^3\left[\Omega_{m0} + \left(1 + \frac{3\omega_0}{1+z}\exp\left(\frac{z}{1+z}\right)\right) \times \Omega_0 \exp(3\omega_0(e^{z/(1+z)} - 1))\right] = 0. \tag{15}$$

IV. DATA FITTING RESULTS

By fitting the model 1 to the combined SN Ia, SDSS, and WMAP data, we get $\Omega_{m0} = 0.25 \pm 0.05$, $\Omega_{k0} = -0.009 \pm 0.05$, and $\omega_0 = -1.1 \pm 0.2$ with $\chi^2 = 175.4$. If we take the model 1 as a unified model of dark energy and dark matter, we find that the best fit parameters to the combined SN Ia, SDSS, and WMAP data are $\Omega_{k0} = -0.05 \pm 0.04$ and $\omega_0 = -0.42 \pm 0.04$ with $\chi^2 = 203.6$. Since $\Delta\chi^2 = 203.6 - 175.4 = 28.2$, we conclude that this model as a unified model of dark matter and dark energy is not a viable model. The contour plots of Ω_{m0} and Ω_{k0} by fixing ω_0 at its best fit value -1.1 are shown in Fig. 2. The contour plots of Ω_{m0} and ω_0 by fixing Ω_{k0} at its best fit value -0.009 are shown in Fig. 3. The evolution of $\omega(z)$ is shown in Fig. 8 (below). Substitute the best fit values to Eq. (11); we get the transition redshift $z_{\mathrm{T}} = 0.56$. The results are summarized in Table I.

If we use SN Ia only, then we get $\Omega_{m0} = 0.33^{+0.3}_{-0.22}$, $\Omega_{k0} = -0.33^{+1.19}_{-0.32}$, and $\omega_0 = -7.5^{+6.9}_{-33.8}$ with $\chi^2 = 171.9$.

By fitting the model 2 to the combined SN Ia, SDSS, and WMAP data, we get $\Omega_{m0} = 0.28 \pm 0.04$, $\Omega_{k0} = -0.001^{+0.046}_{-0.045}$, and $\omega_0 = -0.97^{+0.17}_{-0.19}$ with $\chi^2 = 176.5$. If we take the model 2 as a unified model of dark energy and dark matter, the best fit parameters to the combined SN Ia,

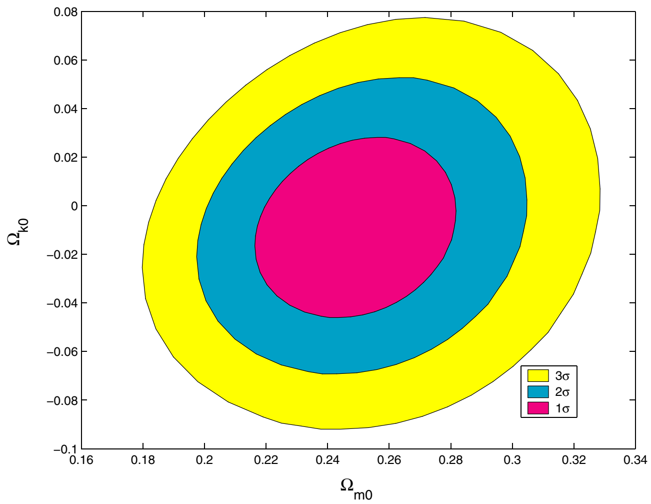

FIG. 2 (color online). The 1σ, 2σ, and 3σ contour plots of Ω_{m0} and Ω_{k0} for the parametrization $\omega = \omega_0/(1+z)$.

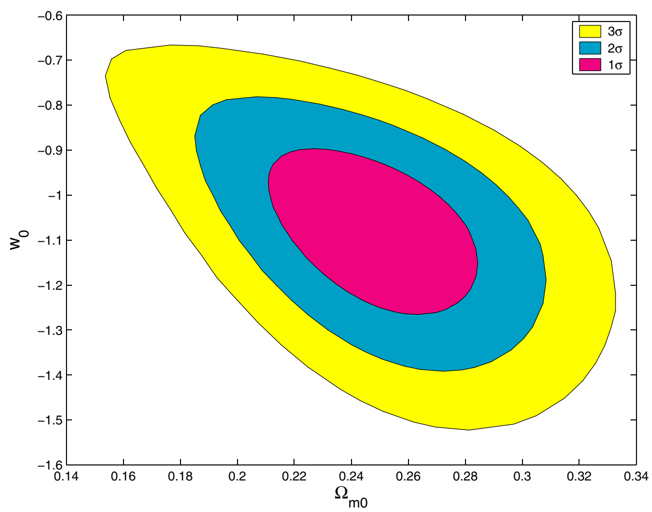

FIG. 3 (color online). The 1σ, 2σ, and 3σ contour plots of Ω_{m0} and ω_0 for the parametrization $\omega = \omega_0/(1+z)$.

SDSS, and WMAP data are $\Omega_{k0} = -0.10 \pm 0.05$ and $\omega_0 = -0.22^{+0.02}_{-0.03}$ with $\chi^2 = 233.2$. Again this model as a unified model of dark matter and dark energy can be firmly ruled out. The contour plots of Ω_{m0} and Ω_{k0} by fixing ω_0 at its best fit value -0.97 are shown in Fig. 4. The contour plots of Ω_{m0} and ω_0 by fixing Ω_{k0} at its best fit value -0.001 are shown in Fig. 5. The evolution of $\omega(z)$ is shown

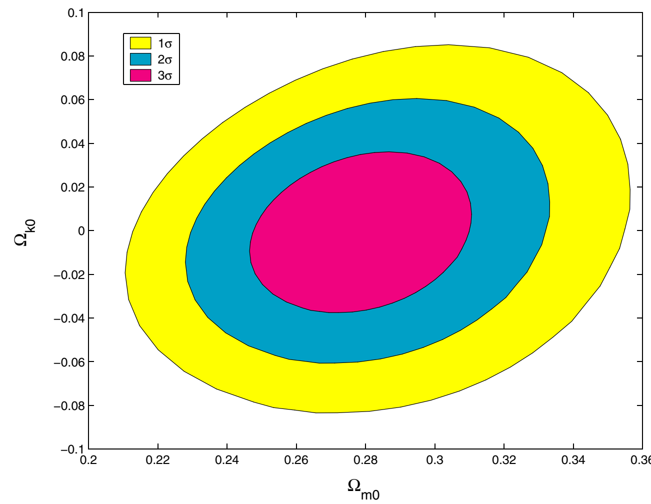

FIG. 4 (color online). The 1σ, 2σ, and 3σ contour plots of Ω_{m0} and Ω_{k0} for the parametrization $\omega = \omega_0 \exp(z/(1+z))/(1+z)$.

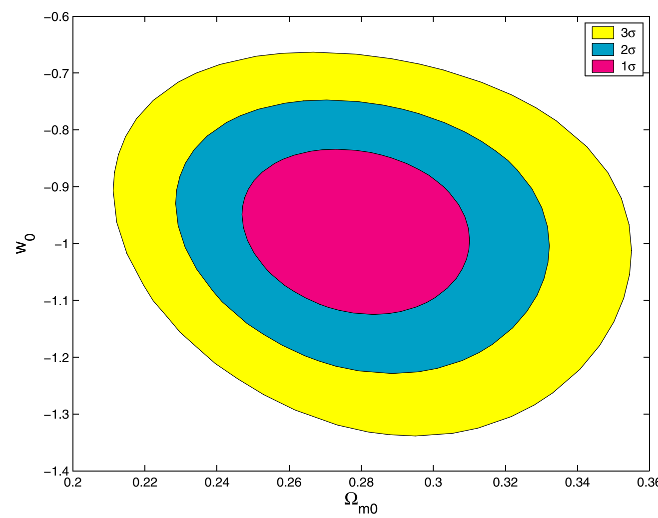

FIG. 5 (color online). The 1σ, 2σ, and 3σ contour plots of Ω_{m0} and ω_0 for the parametrization $\omega = \omega_0 \exp(z/(1+z))/(1+z)$.

in Fig. 8 (below). Substitute the best fit values to Eq. (15), we get the transition redshift $z_T = 0.66$. The results are also shown in Table I.

If we use SN Ia only, then we get $\Omega_{m0} = 0.33_{-0.20}$, $\Omega_{k0} = -0.34^{+1.19}_{-0.32}$, and $\omega_0 = -7.4^{+6.8}_{-33.4}$ with $\chi^2 = 171.9$.

TABLE I. Summary of the best fit parameters.

Model	Ω_{m0}	Ω_{k0}	ω_0	ω_a	z_T	χ^2
1	0.25 ± 0.05	-0.009 ± 0.050	-1.1 ± 0.2	N/A	0.56	175.4
2	0.28 ± 0.04	$-0.001^{+0.046}_{-0.045}$	$-0.97^{+0.17}_{-0.19}$	N/A	0.66	176.5
3	0.28 ± 0.04	N/A	$-1.13^{+0.35}_{-0.26}$	$0.95^{+0.60}_{-1.95}$	0.56	175.62
4	$0.25^{+0.06}_{-0.04}$	N/A	$-1.26^{+0.49}_{-0.44}$	$-2.71^{+4.54}_{-3.12}$	0.69	175.33

Although the two models discussed in the previous section have very different future behavior, they both fit the current data as well as the ΛCDM model. This may suggest that the current data fitting method cannot distinguish models with very different future behavior. The best fit results also show that the Universe is almost spatially flat, and that the best fit results using the combined SN Ia, SDSS, and WMAP data are different from those using SN Ia alone.

V. TWO-PARAMETER PARAMETRIZATION

In this section, we consider spatially flat cosmology only.

Model 3: We first consider the parametrization [10,11]

$$\omega = \omega_0 + \frac{\omega_a z}{1+z}. \tag{16}$$

When $z \gg 1$, we have $\omega \sim \omega_0 + \omega_a$. $\omega \to \pm\infty$ when $z \to -1$. Combining Eqs. (7) and (16), we get the dark energy density

$$\Omega = \Omega_0 (1+z)^{3(1+\omega_0+\omega_a)} \exp(-3\omega_a z/(1+z)), \tag{17}$$

where $\Omega_0 = 1 - \Omega_{m0} - \Omega_{r0}$. Substitute Eqs. (16) and (17) into Eq. (8) and neglect the radiation contribution; we find that z_T satisfies the following equation:

$$\Omega_{m0} + (1-\Omega_{m0})\left(1 + 3\omega_0 + \frac{3\omega_a z}{1+z}\right)(1+z)^{3(\omega_0+\omega_a)} \times \exp\left(\frac{-3\omega_a z}{1+z}\right) = 0. \tag{18}$$

The best fit to the combined SN Ia, SDSS, and WMAP data gives $\omega_0 = -1.13^{+0.35}_{-0.26}$, $\omega_a = 0.95^{+0.60}_{-1.95}$, and $\Omega_{m0} = 0.28 \pm 0.04$ with $\chi^2 = 175.62$. Substitute the best fit parameters into Eq. (18); we get $z_T = 0.56$. The results are summarized in Table I. The contour plots of ω_0 and ω_a by fixing Ω_{m0} at its best fit value 0.28 are shown in Fig. 6. The evolution of $\omega(z)$ is shown in Fig. 8 (below).

Model 4: Next we consider the following parametrization [14]:

$$\omega = \omega_0 + \frac{\omega_a z}{(1+z)^2}. \tag{19}$$

When $z \gg 1$, we have $\omega \sim \omega_0$. When $z \to -1$, we have $\omega \to \pm\infty$. Substitute Eq. (19) into Eq. (7), we get the dark energy density

$$\Omega(z) = \Omega_0 (1+z)^{3(1+\omega_0)} \exp(3\omega_a z^2/2(1+z)^2). \tag{20}$$

Substitute the above two equations (19) and (20) into Eq. (8) and neglect the radiation contribution; we find that z_T satisfies the following equation:

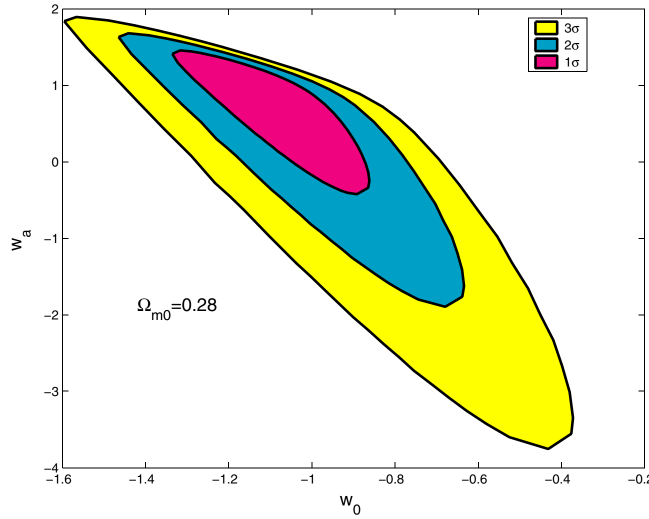

FIG. 6 (color online). The contour plot of ω_0 and ω_a for the parametrization $\omega = \omega_0 + \omega_a z/(1+z)$.

$$\Omega_{m0} + (1-\Omega_{m0})\left(1 + 3\omega_0 + \frac{3\omega_a z}{(1+z)^2}\right)(1+z)^{3\omega_0} \times \exp\left(\frac{3\omega_a z^2}{2(1+z)^2}\right) = 0. \tag{21}$$

The best fit to the combined SN Ia, SDSS, and WMAP data gives $\omega_0 = -1.26^{+0.49}_{-0.44}$, $\omega_a = -2.71^{+4.54}_{-3.12}$, and $\Omega_{m0} = 0.25^{+0.06}_{-0.04}$ with $\chi^2 = 175.33$. Substitute the best fit parameters into Eq. (21), we get $z_T = 0.69$. The results are summarized in Table I. The contour plots of ω_0 and ω_a by fixing Ω_{m0} at its best fit value 0.25 are shown in Fig. 7. The evolution of $\omega(z)$ is shown in Fig. 8.

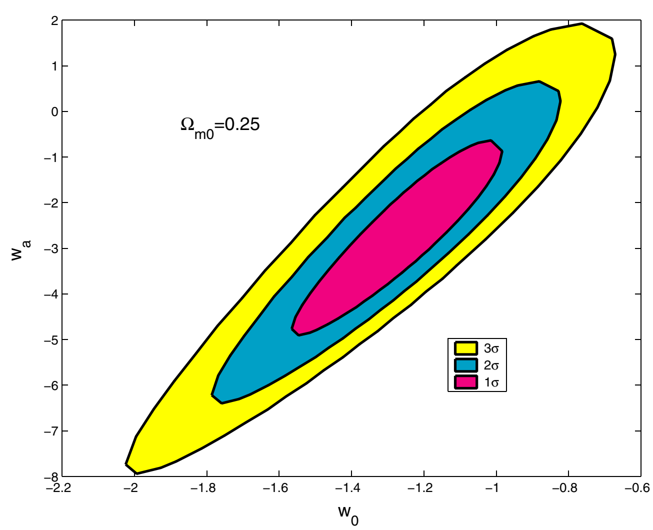

FIG. 7 (color online). The contour plot of ω_0 and ω_a for the parametrization $\omega = \omega_0 + \omega_a z/(1+z)^2$.

VI. DISCUSSION

We discussed two one-parameter dark energy parametrizations and two two-parameter dark energy parametrizations. For the two one-parameter dark energy parametrizations, we consider curved cosmology, so that we have a total of three cosmological parameters: Ω_{m0}, Ω_{k0}, and ω_0. For the two two-parameter dark energy parametrizations, we consider flat cosmology only, again there are three cosmological parameters: Ω_{m0}, ω_0, and ω_a. These different classes of three cosmological parameter models fit the observational data almost equally well because they have almost the same minimum value of χ^2 as shown in Table I. However, they have very different behavior. At early times, the Universe is dominated by matter or radiation, the dark energy is subdominant, so the contribution of dark energy to the background evolution is not important and the data may not be used to distinguish the early behavior of dark energy to the zeroth order. From Fig. 8, we see that the future behavior of $\omega(z)$ is also very different. For the model 1, $\omega(z) \to -\infty$ in the future. For the model 2, $\omega(z) \sim 0$ in the future. For the model 3, $\omega(z) \to -\infty$ in the future. For the model 4, $\omega(z) \to +\infty$ in the future. So the data may not used to distinguish the future behavior of dark energy to the zeroth order either. We need to invoke at least the linear perturbation method to discuss dark energy models. In [37], the authors use the concept of the minimal antitrapped surface or the assumption that the energy momentum content of the observable Universe does not change significantly in comoving coordinates to study the fate of our universe. They found that it is impossible to confirm the accelerating expansion with current observed dark energy value $\Omega_0 \sim 0.7$ if the dark energy is not a phantom. These results more or less support our conclusion. The dark energy in the models 1 and 2 tracked the matter in the past. The two models both suggest that the Universe is almost spatially flat. All the models suggest that $z_T \sim 0.6$ and $\omega(0) \sim -1$. These results are consistent with those derived from the simplest ΛCDM model. However, it was found that $z_T \sim 0.3$ by using SN Ia data only [15]. So the results by using combined SN Ia, SDSS, and WMAP data are different from those by using SN Ia data only. More thorough studies are needed to make more concise conclusion. Finally, we would like to mention that the one- and two-parameter representations of dark energy models have their own limitations as discussed in [38]. These parametrizations do not accommodate the possibility of rapid evolution of dark energy.

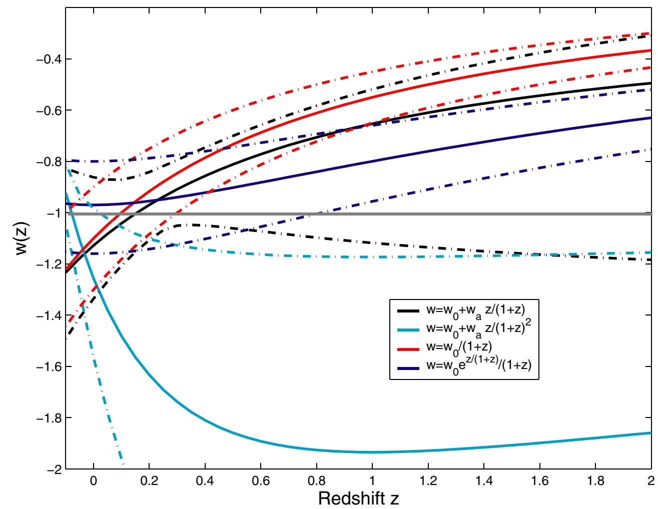

FIG. 8 (color online). The behavior of $\omega(z)$. The solid lines plot $\omega(z)$ by using the best fit parameters and the dash dotted lines are for 1σ errors. For the two-parameter representations, the 1σ errors are obtained from the 1σ contours of ω_0 and ω_a.

ACKNOWLEDGMENTS

Y. Gong is supported by CQUPT under Grant No. A2004-05, NNSFC under Grant No. 10447008, CSTC under Grant No. 2004BB8601, and SRF for ROCS, State Education Ministry. Y. Z. Zhang's work was in part supported by NNSFC under Grant No. 90403032 and also by National Basic Research Program of China under Grant No. 2003CB716300.

[1] S. Perlmutter *et al.*, Astrophys. J. **517**, 565 (1999).
[2] P. M. Garnavich *et al.*, Astrophys. J. **493**, L53 (1998)
[3] A. G. Riess *et al.*, Astron. J. **116**, 1009 (1998).
[4] V. Sahni and A. A. Starobinsky, Int. J. Mod. Phys. D **9**, 373 (2000).
[5] T. Padmanabhan, Phys. Rep. **380**, 235 (2003).
[6] J. Weller and A. Albrecht, Phys. Rev. Lett. **86**, 1939 (2001).
[7] D. Huterer and M. S. Turner, Phys. Rev. D **64**, 123527 (2001).
[8] J. Weller and A. Albrecht, Phys. Rev. D **65**, 103512 (2002).
[9] P. Astier, Phys. Lett. B **500**, 8 (2001).
[10] M. Chevallier and D. Polarski, Int. J. Mod. Phys. D **10**, 213 (2001).
[11] E. V. Linder, Phys. Rev. Lett. **90**, 91301 (2003).
[12] T. R. Choudhury and T. Padmanabhan, Astron. Astrophys. **429**, 807 (2005).
[13] B. Feng, X. L. Wang, and X. M. Zhang, Phys. Lett. B **607**, 35 (2005).
[14] H. K. Jassal, J. S. Bagla, and T. Padmanabhan, Mon. Not. R. Astron. Soc. **356**, L11 (2005).
[15] Y. Gong, Classical Quantum Gravity **22**, 2121 (2005).
[16] G. Efstathiou, Mon. Not. R. Astron. Soc. **310**, 842 (1999)

[17] B. F. Gerke and G. Efstathiou, Mon. Not. R. Astron. Soc. **335**, 33 (2002).
[18] P.S. Corasaniti and E.J. Copeland, Phys. Rev. D **67**, 063521 (2003).
[19] C. Wetterich, Phys. Lett. B **594**, 17 (2004).
[20] U. Alam, V. Sahni, T.D. Saini, and A.A. Starobinsky, Mon. Not. R. Astron. Soc. **354**, 275 (2004).
[21] U. Alam, V. Sahni, and A.A. Starobinsky, J. Cosmol. Astropart. Phys. 06 (2004) 008.
[22] R.A. Daly and S.G. Djorgovski, Astrophys. J. **597**, 9 (2003).
[23] R.A. Daly and S.G. Djorgovski, Astrophys. J. **612**, 652 (2004).
[24] Y. Gong, Int. J. Mod. Phys. D **14**, 599 (2005).
[25] J. Jönsson, A. Goobar, R. Amanullah, and L. Bergström, J. Cosmol. Astropart. Phys. 09 (2004) 007.
[26] Y. Wang and P. Mukherjee, Astrophys. J. **606**, 654 (2004).
[27] Y. Wang and M. Tegmark, Phys. Rev. Lett. **92**, 241302 (2004).
[28] V.F. Cardone, A. Troisi, and S. Capozziello, Phys. Rev. D **69**, 083517 (2004).
[29] D. Huterer and A. Cooray, Phys. Rev. D **71**, 023506 (2005).
[30] A.G. Riess *et al.*, Astrophys. J. **607**, 665 (2004).
[31] D.J. Eisenstein *et al.*, astro-ph/0501171 [Astrophys. J. (to be published)].
[32] C.L. Bennett *et al.*, Astrophys. J. Suppl. Ser. **148**, 1 (2003).
[33] H.B. Sandvik, M. Tegmark, M. Zaldarriaga, and I. Waga, Phys. Rev. D **69**, 123524 (2004).
[34] M.C. Bento, O. Bertolami, and A.A. Sen, Phys. Rev. D **70**, 083519 (2004).
[35] R.R.R. Reis, M. Makler, and I. Waga, Classical Quantum Gravity **22**, 353 (2005).
[36] Z.K. Guo, R.G. Cai, and Y.Z. Zhang, J. Cosmol. Astropart. Phys. 05 (2005) 002.
[37] T. Vachaspati and M. Trodden, Phys. Rev. D **61**, 023502 (2000); G. Starkman, M. Trodden, and T. Vachaspati, Phys. Rev. Lett. **83**, 1510 (1999); P.P. Avelino, J.P.M. de Carvalho, and C.J.A.P. Martins, Phys. Lett. B **501**, 257 (2001); D. Huterer, G.D. Starkman, and M. Trodden, Phys. Rev. D **66**, 043511 (2002).
[38] B.A. Bassett, P.S. Corasaniti, and M. Kunz, Astrophys. J. **617**, L1 (2004).